Electron Affinities and Gas-Phase Acidities of Organogermanium and Organotin Compounds

Elizabeth A. Brinkman,† Karen Salomon, William Tumas, and John I. Brauman*

Contribution from the Department of Chemistry, Stanford University, Stanford, California 94305-5080

Received July 11, 1994®

Abstract: The electron affinities have been measured for trimethylgermanium and trimethyltin radicals as 31.9 ± 0.7 and 39.2 ± 1.5 kcal/mol, respectively, using electron photodetachment spectroscopy. The acidities ($\Delta H°_{acid}$) for the corresponding hydrides (Me_3GeH and Me_3SnH) have been bracketed as 361.5 ± 2.8 and 349 ± 2 kcal/mol. From the electron affinities and the acidities, the $D°(Me_3MH)$ are derived as 79.8 ± 3.5 and 75 ± 3.5 kcal/mol, respectively. These physical properties are compared with the properties of the group IVA through group VIIA binary hydrides and methyl-substituted compounds. The electron affinities of the group IVA compounds do not conform to the regular pattern; some of the reasons for this are discussed.

Introduction

The thermochemistry of the group IVA compounds has been most extensively studied for carbon.[1] Much less is known about the thermochemistry of the silicon compounds,[2,3] despite their extensive use as synthetic reagents, as polymers and as precursors in semiconductor manufacturing. Even less is known for germanium and tin compounds. Germane is used for CVD of germanium−silicon films,[4] and numerous organogermanium compounds have been synthesized. Organotin hydrides are extensively used in synthesis as hydrogen donors, because of the relatively weak Sn−H bond.[5]

The electron affinity of the germyl radical, GeH_3, has been measured previously.[6] The M−H bond dissociation energies for germane (GeH_4)[7−11] and stannane (SnH_4)[7,12] have also been measured, although because of the difficulties of these experiments, considerable uncertainty still exists for these values. The acidities of organotin and organogermanium hydrides are unknown.

In this work we have measured the electron affinities for Me_3Ge and Me_3Sn using electron photodetachment spectroscopy and determined the acidities for Me_3GeH and Me_3SnH using bracketing reactions. From these data we derive the corresponding Ge−H and Sn−H bond dissociation energies. We compare these thermochemical values with those of the analogous carbon and silicon compounds, along with the existing data for the hydride species (H_4M).

Experimental Section

Materials. Hexamethyldigermane was purchased from Alfa or synthesized by the reaction of trimethylchlorogermane with magnesium amalgam.[13] Hexamethylditin was purchased from Alfa or Aldrich. Nitrogen trifluoride was purchased from Ozark Mahoning. Before introduction into the high-vacuum chamber, all neutrals were degassed by several freeze−pump−thaw cycles on the foreline.

Ion Generation. Fluoride ion was generated by the dissociative electron capture of nitrogen trifluoride, NF_3.

$$NF_3 + e^- \rightarrow F^- + NF_2 \quad (1)$$

Trimethylgermanium and trimethyltin anions were then generated by the nucleophilic displacement by fluoride ion of the digermanium or ditin compound.

$$F^- + Me_3GeGeMe_3 \rightarrow Me_3Ge^- + Me_3GeF \quad (2)$$

$$F^- + Me_3SnSnMe_3 \rightarrow Me_3Sn^- + Me_3SnF \quad (3)$$

These reactions are modeled on the work of DePuy and co-workers,[14,15] which uses the reaction of trimethylsilyl derivatives with fluoride ion to displace anions of interest. Nucleophilic displacement of trimethylgermanium and trimethyltin also appears to be a general method for the generation of germanium and tin anions. Because of the multiple isotopes present for both germanium and tin, at least three difference masses were generated for each anion. Isotopic resolution was verified before collection of data and the mass of highest abundance was used, $Me_3{}^{74}Ge$ and $Me_3{}^{120}Sn$ anion, respectively.

Electron Photodetachment Experiments. (a) Instrumental. Experiments were performed in an ion cyclotron resonance (ICR) spectrometer operating in the CW mode,[16] which allows continuous ion generation and detection. The signal-to-noise ratio obtained with CW ICR is ideal for measuring small changes in the ion population (<1%). Single-frequency phase-sensitive detection was accomplished

† Current address: Molecular Physics Department, SRI International, Menlo Park, CA 94025.

® Abstract published in *Advance ACS Abstracts,* March 15, 1995.

(1) Lias, S. G.; Bartmess, J. E.; Holmes, J. L.; Levin, R. D.; Liebman, J. F.; Mallard, W. G. *J. Phys. Chem. Ref. Data* **1988**, *17*, Suppl. 1.

(2) Wetzel, D. M.; Salomon, K. E.; Berger, S.; Brauman, J. I. *J. Am. Chem. Soc.* **1989**, *111*, 3835−3841.

(3) Walsh, R. In *The Chemistry of Organic Silicon Compounds*; Patai, S., Rappoport, Z., Ed.; John Wiley and Sons Ltd.: New York, 1989; Vol. I, pp 371−391.

(4) Arienzo, M.; Iyer, S. S.; Meyerson, B. S.; Patton, G. L.; Stork, J. M. C. *Appl. Surf. Sci.* **1991**, *48/49*, 377−386.

(5) March, J. *Advanced Organic Chemistry: Reactions, Mechanisms, and Structure*, 3rd ed.; Wiley Interscience: New York, 1985.

(6) Reed, K. J.; Brauman, J. I. *J. Chem. Phys.* **1974**, *61*, 4830−4838.

(7) Jackson, R. A. *J. Organomet. Chem.* **1979**, *166*, 17−19.

(8) Doncaster, A. M.; Walsh, R. *J. Phys. Chem.* **1979**, *83*, 578−581.

(9) Noble, P. N.; Walsh, R. *Int. J. Chem. Kinet.* **1983**, *15*, 547−560.

(10) Agrawalla, B. S.; Setser, D. W. *J. Chem. Phys.* **1987**, *86*, 5421−5432.

(11) Clark, K. B.; Griller, D. *Organometallics* **1991**, *10*, 746−750.

(12) Burkey, T. J.; Majewski, M.; Griller, D. *J. Am. Chem. Soc.* **1986**, *108*, 2218−2221.

(13) Triplett, K.; Curtis, M. D. *J. Organomet. Chem.* **1976**, *107*, 23−32.

(14) DePuy, C. H.; Bierbaum, V. M.; Flippin, L. A.; Grabowski, J. J.; King, G. K.; Schmitt, R. J. *J. Am. Chem. Soc.* **1979**, *101*, 6443.

(15) DePuy, C. H.; Bierbaum, V. M.; Flippin, L. A.; Grabowski, J. J.; King, G. K.; Schmitt, R. J.; Sullivan, S. A. *J. Am. Chem. Soc.* **1980**, *102*, 5012−5015.

(16) Lehman, T. A.; Bursey, M. M. *Ion Cyclotron Resonance Spectrometry*; Wiley-Interscience: New York, 1976.

0002-7863/95/1517-4905$09.00/0

using home-built capacitance bridge detection (CBD) circuitry,[17] together with a commercial lock-in amplifier (Princeton Applied Research Corp., Model 124A). The voltage output from the CBD is proportional to the number of ions in the ICR cell.[18] A frequency-lock system[17] was employed to correct for frequency shifts (typically ±0.1 kHz in 150 kHz) induced during photochemical experiments.

(b) Light Sources. The ions were irradiated with light from an arc lamp or a dye laser. Low-resolution spectra were obtained using a 1000-W xenon arc lamp (Canrad-Hanovia) in conjunction with a 0.25-m high-intensity-grating monochromator (Kratos Analytical). Lamp power was measured using a thermopile (Eppley Laboratory, Inc.). Because of the configuration of our experimental setup, arc lamp power measurements could not be performed simultaneously with the electron photodetachment data collection and were obtained separately.

A dye laser (Coherent 590), pumped by a Coherent argon ion laser (Innova 200/15), was used to irradiate the ions. Wavelengths were selected with a three-plate birefringent filter; the spectral bandwidth was typically 1 cm^{-1}. Laser dyes (Exciton) used and wavelength ranges include the following: DCM (605−705 nm), LDS 698 (670−750 nm), and LDS 821 (800−885 nm). The dye laser was calibrated by using the optogalvanic effect.[19,20] The output from the dye laser is introduced into a Ca/Ne hollow cathode lamp and the current of the lamp is monitored as the laser is tuned. The current changes if the laser is tuned to an electronic transition of the species in the lamp. The dye laser was calibrated using the known transitions for these elements.[21] Dye laser power was measured simultaneously with data collection by splitting off a small portion of the beam and directing it into a thermopile (Eppley Laboratory, Inc.).

(c) Data Acquisition and Processing. Electron photodetachment experiments were performed by monitoring the anion population (A^-) as a function of the wavelength (energy) of irradiation.

$$A^- + h\nu \rightarrow A + e^- \qquad (4)$$

Data collection typically involved measuring the ion intensity without light at the beginning and the end of a scan and collecting signal measurements at 10−100 consecutive steps; the signal was measured and averaged for 3 to 5 s at each step and step sizes were typically 12 nm for the arc lamp spectra or less than 1.5 nm for the dye laser spectra. The relative cross section, $\sigma(\lambda)$, was calculated from the fractional ion signal change, $F(\lambda)$, the wavelength, λ, and the energy of the light at that wavelength, $E(\lambda)$, using the steady state model:[22]

$$\sigma(\lambda) = \frac{F(\lambda)}{\lambda E(\lambda)(1 - F(\lambda))} \qquad (5)$$

A minimum of three scans were averaged together for each wavelength region. Each laser photodetachment spectrum was comprised of several small, overlapping wavelength regions, spliced together.

Acidity Measurements. Instrumental. Acidity bracketing was performed using an ICR spectrometer operating in the pulsed mode.[23] Ion concentrations were monitored using a capacitance bridge detection system that was channeled into a boxcar averager and interfaced to a computer (IBM XT). This computer was used to acquire and analyze data as well as to control the timing circuitry during the experiment. The time dependence of the concentration of a specific ion was monitored by moving the detect pulse relative to the grid pulse at a fixed magnetic field and frequency. Reaction pathways were verified using double-resonance techniques involving the ejection of selected ions. Operating pressures were typically 10^{-7} to 10^{-6} Torr and were measured using a vacion gauge (Varian UHV-24) which was calibrated using a capacitance manometer (MKS Baratron) at 10^{-5} Torr.

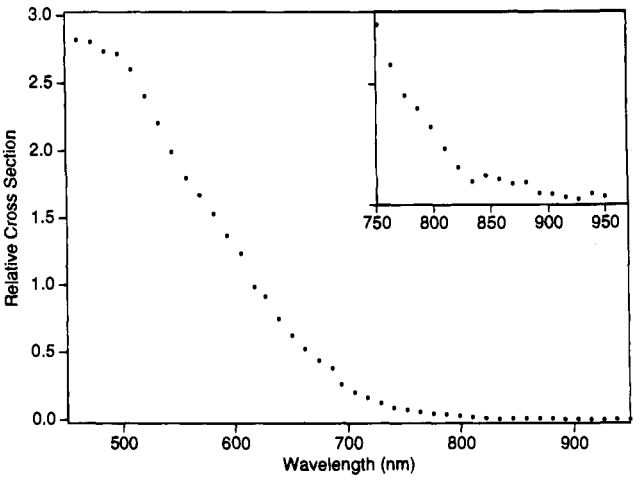

Figure 1. Low-resolution electron photodetachment spectrum for the $Me_3{}^{74}Ge$ anion, bandwidth = 40 nm fwhm. The inset shows an expanded view of the threshold.

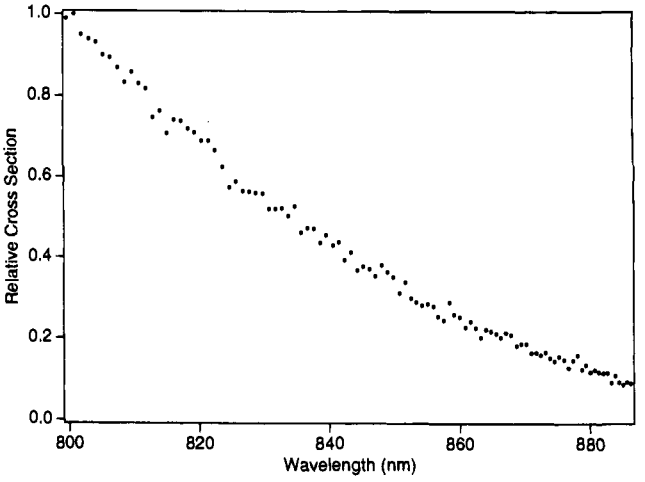

Figure 2. High-resolution electron photodetachment spectrum for the $Me_3{}^{74}Ge$ anion.

Results

Photodetachment Spectra. The photodetachment spectra obtained are shown in Figures 1−4. All spectra show cross sections that are smoothly increasing functions above threshold. The cross section at any particular wavelength is the sum of all available transitions from the ground state anion to the various rotational, vibrational, and electronic states of the neutral and excited electronic states of the anion. Transitions to these excited states will be superimposed on the background detachment and will appear as slope changes in the spectrum.

The threshold for photodetachment is the energy at which the cross section first rises from zero. This threshold is generally assigned as the adiabatic electron affinity for the radical, presuming that the Franck−Condon factors for the $v'' = 0 \rightarrow v' = 0$ transition are strong enough to be observed and that hot band transitions are unimportant.

Ab initio calculations predict that fourth period hydride anions (H_3M) undergo geometry changes upon photodetachment to the neutral.[24,25] The geometry changes in the Me_3M anions upon photodetachment, however, are unknown. Substantial geometry changes upon photodetachment would complicate the determi-

(17) Marks, J.; Drzaic, P. S.; Foster, R. F.; Wetzel, D. M.; Brauman, J. I.; Uppal, J. S.; Staley, R. H. *Rev. Sci. Instrum.* **1987**, *58*, 1460−1463.
(18) McIver, R. T., Jr.; Ledford, E. B., Jr.; Hunter, R. L. *J. Chem. Phys.* **1980**, *72*, 2535.
(19) King, D. S.; Schenck, P. K.; Smyth, K. C.; Travis, J. C. *Appl. Opt.* **1977**, *16*, 2617−2619.
(20) King, D. S.; Schenck, P. K. *Laser Focus* **1978**, *3*, 50−57.
(21) *M.I.T. Wavelength Tables—Wavelengths by Element*; M.I.T. Press: Cambridge, 1982; Vol. 2.
(22) Zimmerman, A. H. Ph.D. Thesis, Stanford University, 1977.
(23) Moylan, C. R.; Jasinski, J. M.; Brauman, J. I. *J. Am. Chem. Soc.* **1985**, *107*, 1934−1940.
(24) Eades, R. A.; Dixon, D. A. *J. Chem. Phys.* **1980**, *72*, 3309−3313.
(25) Ortiz, J. V. *J. Am. Chem. Soc.* **1987**, *109*, 5072−5076.

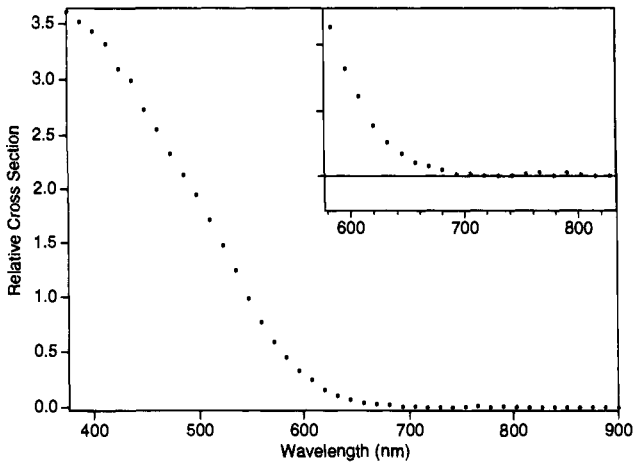

Figure 3. Low-resolution electron photodetachment spectrum for the $Me_3{}^{120}Sn$ anion, bandwidth = 40 nm fwhm. The inset shows an expanded view of the threshold.

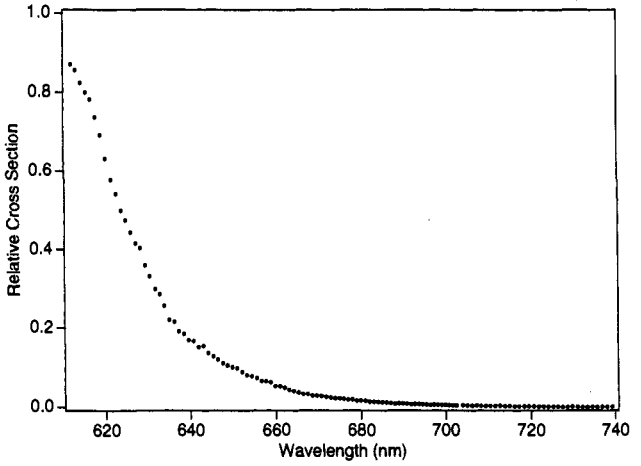

Figure 4. High-resolution electron photodetachment spectrum for the $Me_3{}^{120}Sn$ anion.

nation of the adiabatic threshold. Previous photodetachment studies of various substituted silyl anions suggest that this has not prevented the assignment of the adiabatic electron affinity for those radicals.[2] Because the calculated geometry changes for silyl and germyl anions are similar, we do not expect that geometry changes will obscure the determination of the adiabatic electron affinities in this case either. The geometry changes for the tin system have not previously been calculated to our knowledge.

The photodetachment thresholds for both ions display very slowly rising cross sections, followed by steeply rising cross sections. Predictions regarding the slope of the photodetachment spectrum at threshold can be made based on the type of orbital from which the electron is removed.[26] *Ab initio* studies predict that silyl and germyl anions are quite pyramidal (H−M−H angle = 95−98°),[24,25] leading us to predict that the extra electron resides in an orbital with substantial s character. The detached electron is therefore expected to be a p wave, which should show a cross section whose slope is proportional to $E^{3/2}$, where E is the energy of the ejected electron.[26] Therefore, the cross section is expected to rise slowly, and we believe that the onset of the slowly rising cross section actually corresponds to the adiabatic electron affinity. Onsets were assigned using two methods. The first involved a linear extrapolation of the data to zero cross section. The second method involved taking the derivative of a smoothed cubic spline function determined from a least-squares fit of the data.[27] The onset assignments are discussed in more detail for the individual ions.

(a) Trimethylgermanium. The low-resolution photodetachment spectrum for the trimethylgermanium anion is shown in Figure 1. We observe a smooth, slowly rising cross section, with an onset at 920 nm. To correct for the monochromator bandwidth, the bandwidth (40 nm fwhm) was subtracted from this onset, yielding a bandwidth corrected onset of 880 ± 40 nm (32.5 ± 1.5 kcal/mol). Below 700 nm the cross section rises sharply and appears to level off around 500 nm, suggesting cross section enhancement as a result of an excited state of the anion, although we do not see an absorption maximum. The electronic absorption spectra in solution for several trimethylgermyl alkali metal compounds show a maximum ca. 280−300 nm,[28] consistent with our observation that the absorption maximum is below 450 nm.

To refine the electron affinity assignment, this anion was photodetached using a dye laser (Figure 2). Experimental limitations of the laser prevented observation of detachment above 885 nm, so the threshold was not actually observed. We extrapolate the observed spectrum to zero cross section and obtain an onset of 897 nm. Because we have not observed the actual threshold, we assign a correspondingly large error limit of ±20 nm, yielding an electron affinity of 31.9 ± 0.7 kcal/mol.

(b) Trimethyltin. The low-resolution photodetachment spectrum for this ion is shown in Figure 3. The trimethyltin anion electron photodetachment spectrum is quite similar to that observed for the trimethylgermanium anion. Again we see a smooth, slow-rising cross section, with the onset observed at 720 nm. Subtraction of the bandwidth (40 nm fwhm) yields a bandwidth corrected onset of 680 ± 40 nm (42.0 ± 2.7 kcal/mol). Below 600 nm the spectrum rises sharply, suggesting enhancement of the spectrum due to an excited electronic state which lies in the continuum.

The high-resolution spectrum (Figure 4) displays a very slowly rising cross section, with an onset of 730 nm (39.2 kcal/mol). This onset is outside the expected range from the low-resolution spectrum. This low-energy tail observed in the laser experiments may result from poor Franck−Condon factors, as a result of geometry changes which would cause the onset to appear at shorter wavelength (higher energy) than the adiabatic threshold; the higher intensity of the laser experiments would facilitate the observation of such a band. It may also be a result of a hot band which would cause the onset to appear at longer wavelengths (lower energy) than the adiabatic threshold. From our experience with silyl anions which we expect to have similar geometry changes and with the hot bands observed in previous photodetachment work, we do not expect these to contribute more than ±1.5 kcal/mol. Therefore, we assign the electron affinity as 39.2 ± 1.5 kcal/mol.

Acidity Bracketing. The acidities of trimethylgermanium hydride and trimethyltin hydride were determined using the bracketing technique.[29,30] The Me_3M anions were generated by reaction of fluoride with the digermanium or ditin compound. Because the parent hydrides (Me_3GeH and Me_3SnH) were not present, equilibrium measurements could not be carried out and the acidity could only be bracketed. The conjugate base of the

(26) Reed, K. J.; Zimmerman, A. H.; Andersen, H. C.; Brauman, J. I. *J. Chem. Phys.* **1976**, *64*, 1368−1375.

(27) Janousek, B. K. Ph.D. Thesis, Stanford University, 1979.

(28) Mochida, K.; Kugita, T.; Nakadaira, Y. *Polyhedron* **1990**, *9*, 2263−2266.

(29) Pellerite, M. J.; Jackson, R. L.; Brauman, J. I. *J. Phys. Chem.* **1981**, *85*, 1624−1626.

(30) Baer, S.; Brinkman, E. A.; Brauman, J. I. *J. Am. Chem. Soc.* **1991**, *113*, 805−812.

Table 1. Results of Bracketing Studies[a]

reaction	$\Delta G°_{acid}$[b]	reaction obsd
Me_3Ge^- + MeSH	350.6 ± 2	yes
Me_3Ge^- + *m*-fluoroaniline	353.9 ± 2	yes
Me_3Ge^- + *o*-fluoroaniline	355.3 ± 2	no
Me_3Sn^- + 2,4-pentanedione	336.6 ± 2.0	yes
Me_3Sn^- + HCO_2H	338.3 ± 2.0	yes
Me_3Sn^- + $EtCO_2H$	340.4 ± 2.0	yes
Me_3Sn^- + $MeCO_2H$	341.5 ± 2.0	yes
Me_3Sn^- + PhOH	342.3 ± 2.0	no
Me_3Sn^- + H_2S	344.8 ± 2.0	no

[a] All values in kcal/mol. [b] All acidity values from ref 33.

Table 2. Acidities and Electron Affinities[a]

R	$\Delta G°_{acid}$(R−H)	$\Delta S°_{acid}$(R−H)[b]	$\Delta H°_{acid}$(R−H)	EA(R)
Me_3Ge	355 ± 3	24.4	362 ± 3	31.9 ± 0.7
Me_3Sn	342 ± 2	24.4	349 ± 2	39.2 ± 1.5

[a] All values in kcal/mol, except as noted. [b] cal deg^{-1} $mole^{-1}$. Based on models (see text).

acid (Me_3Ge^- or Me_3Sn^-) was generated in the presence of a neutral gas for which the acidity was known (HA). The reference acids used for the bracketing were all more acidic than HF, and therefore could also be deprotonated by F^-, also generating A^-.

$$F^- + AH \rightarrow FH + A^- \quad (6)$$

$$Me_3M^- + AH \rightarrow Me_3MH + A^- \quad (7)$$

To verify whether the A^- was produced from reaction 6 or 7, Me_3M^- was ejected from the cell using double-resonance techniques and the time evolution of A^- was monitored. A decrease in the production of A^- upon ejection implies that Me_3M^- deprotonates AH and that Me_3MH is less acidic than AH. Thus $\Delta G°_{acid}(Me_3MH) > \Delta G°_{acid}(AH)$. If Me_3M^- does not deprotonate AH then the A^- production should not be affected by ejection of Me_3M^-. In this case Me_3MH is more acidic than AH ($\Delta G°_{acid}(Me_3MH) < \Delta G°_{acid}(AH)$). This bracketing process is repeated using a series of reference acids until the upper and the lower acidity limits are found.

The results of the acidity bracketing are summarized in Table 1; the assigned acidities are reported in Table 2. The uncertainties in $\Delta G°_{acid}$ are a reflection of the uncertainties in the reference acids as well as the uncertainty due to bracketing. $\Delta S°_{acid}$ values are taken as 24.4 cal deg^{-1} mol^{-1}, consistent with that found for similar acids.[2]

Discussion

The electron affinities, acidities, and bond dissociation energies for the hydrides (MH_4) and trimethyl hydrides (Me_3MH) are summarized in Table 3. The M−H bond dissociation energies for Me_3GeH and Me_3SnH are derived from the acidity and electron affinity data. To understand the periodic trends of column IVA, we compare the properties of the hydride compounds (CH_4, SiH_4, etc.) with the hydrides of columns VA through VIIA. Because SnH_4 is not stable at room temperature, the acidity and electron affinity of SnH_3 were not determined. Following a discussion of the periodic trends for electron affinities, bond dissociation energies, and acidities of the hydride compounds, the properties of the methyl-substituted compounds are compared.

Electron Affinities. A comparison of main group electron affinities could include a comparison of the electron affinities of the bare atoms, but the electron occupancy of partially filled shells affects the stability of the species, making changes from atom to atom difficult to interpret. A comparison of the electron affinities of the ligated atoms allows a comparison of the isoelectronic species. Because ligands define a geometry about the central atom, however, the geometry may be different in the anion and the neutral, also making electron affinity comparisons difficult to interpret. When we remove an electron from the anion, the bonding to the ligands can change, depending on the electronic structure and geometry of the anion and neutral. The adiabatic electron affinity reflects the total energy change for the system, including changes in bonding to the ligands. Interestingly, as deduced from secondary isotope effects,[31] the change from CH_3 to CH_3^- should result in increased zero-point energy associated with the C−H bonds and thus give a higher adiabatic EA than would have been the case if there were no change in the C−H bonds.

Table 3. Acidities, Electron Affinities, and Bond Energies of Group IVA Compounds[a]

R−H	$\Delta H°_{acid}$(R−H)	EA(R)	$D°$(R−H)
CH_4	417[b]	1.8[c]	104.8[d]
Me_3CH	413.1 ± 1[e]	−3.1[f]	96.4 ± 0.4[g]
SiH_4	372.8 ± 2[h]	32.4 ± 0.6[h]	90.3 ± 1.2[j]
		32.4 ± 0.3[i]	91.9 ± 0.5[k]
Me_3SiH	383 ± 3[l]	22.4 ± 0.6[h]	90.3 ± 1.4[j]
GeH_4	359.0 ± 1.2[m]	40.1 ± 0.9[n]	78.0 ± 1[o]
			82.6 ± 2.4[p]
			83.2 ± 1.9[q]
			85.5 ± 2.2[m]
Me_3GeH	361.5 ± 2.8	31.9 ± .7	79.8 ± 3.5
			82[r]
			81.7 ± 2.4[s]
			81.6 ± 0.5[t]
Me_3SnH	349 ± 2	39.2 ± 1.5	75 ± 3.5
			74[r]
			73.7 ± 2[u]

[a] All values in kcal/mol. Values are from this work unless otherwise noted. [b] Reference 33. [c] Reference 37. [d] Reference 52. [e] Derived from the acidity and the bond dissociation energy. [f] Reference 48. [g] Reference 57. [h] Reference 2. [i] Reference 38. [j] Reference 53. [k] Reference 58. [l] Reference 55. [m] 298 K value. Reference 56. [n] Reference 6. [o] Reference 10. [p] Reference 9. [q] 0 K value. Reference 59. [r] Estimated from appearance potentials in ref 7. [s] Reference 8. [t] Reference 11. [u] $D°$(Sn−H) for Bu_3SnH.[12] We expect this to be quite similar to that for Me_3SnH.

In columns VA through VIIA of the periodic table,[6,32,33] the electron affinities of the binary hydrides generally increase down the column from row 1 to row 2, but remain essentially unchanged or decrease slightly for the following rows (e.g., EA(NH_2) = 17.8 kcal/mol,[34] EA(PH_2) = 29.3 kcal/mol,[35] EA(AsH_2)= 29.3 kcal/mol[36]). The column IVA hydrides, however, show a large electron affinity increase down the column. The electron affinity increases dramatically from CH_3 (1.8 kcal/mol[37]) to SiH_3 (32.4 kcal/mol[2,38]), but much less from SiH_3 to GeH_3 (40.1 kcal/mol[6]).

Across a row, the electron affinities always increase for columns VA through VIIA (e.g., EA(NH_2) = 17.8 kcal/mol,[34]

(31) Streitwieser, A., Jr.; Jagow, R. H.; Fahey, R. C.; Suzuki, S. *J. Am. Chem. Soc.* **1958**, *80*, 2327.
(32) Brauman, J. I.; Eyler, J. R.; Blair, L. K.; White, M. J.; Comisarow, M. B.; Smyth, K. C. *J. Am. Chem. Soc.* **1971**, *93*, 6360−6362.
(33) Bartmess, J. E. NIST Negative Ion Energetics Database, Version 3.00; U.S. Department of Commerce, National Institute of Standards and Technology, 1993.
(34) Wickham-Jones, C. T.; Ervin, K. M.; Ellison, G. B.; Lineberger, W. C. *J. Chem. Phys.* **1989**, *91*, 2762−2763.
(35) Zittel, P. F.; Lineberger, W. C. *J. Chem. Phys.* **1976**, *65*, 1236.
(36) Smyth, K. C.; Brauman, J. I. *J. Chem. Phys.* **1972**, *56*, 4620.
(37) Ellison, G. B.; Engelking, P. C.; Lineberger, W. C. *J. Am. Chem. Soc.* **1978**, *100*, 2556−2558.
(38) Nimlos, M. R.; Ellison, G. B. *J. Am. Chem. Soc.* **1986**, *108*, 6522−6529.

EA(OH) = 42.2 kcal/mol,[39] EA(F) = 78.4 kcal/mol;[40] and EA(PH_2) = 29.3 kcal/mol,[35] EA(SH) = 53.4 kcal/mol,[41] EA(Cl) = 83.4 kcal/mol[40]). Again, however, the electron affinities of the column IVA hydrides are anomalous. Between columns IVA and VA the electron affinity increases in the first row (EA(CH_3) = 1.8 kcal/mol,[37] EA(NH_2) = 17.8 kcal/mol[34]), consistent with the trend observed for the other columns, but decreases in the following rows (EA(SiH_3) = 32.4 kcal/mol,[2,38] EA(PH_2) = 29.3 kcal/mol;[35] and EA(GeH_3) = 40.1 kcal/mol,[6] EA(AsH_2) = 29.3 kcal/mol[36]). In short, given the data for columns VA, VIA, and VIIA, we might have expected that the EA's of SiH_3 and GeH_3 should have been substantially smaller.

The anomalous behavior of the electron affinities of the column IVA hydrides is a consequence of symmetry as well as the nature of the central atom. In columns VA, VIA, and VIIA, symmetry requires the most weakly bound electron to be in a nonbonding p orbital. Consistent with the nonbonding character of the anion and the radical, the geometries of the anion and the radical are similar (in the NH_2 radical the H−N−H angle is 103.1° and in the anion the angle is 102.0°;[42] in PH_2 and PH_2^- the H−P−H angle is ~91.7°[35]). The group IVA hydrides show different behavior. In these anions the most weakly bound electron is in an orbital with some bonding character. The 8 electron anion is expected to be pyramidal, while the 7 electron neutral can be planar or pyramidal, depending on the central atom.[43] The methyl anion is calculated to be pyramidal (H−C−H angle = 109−112°, depending on the basis set),[25,44] while the methyl radical is planar. The silyl anion and the radical are both pyramidal:[38] the anion has an angle of 94.5°, while the radical has an angle of 112.5°. The bond angles in the germyl anion and the radical are calculated using *ab initio* methods to be similar to those in the silyl system:[25] the anion angle is 93−96° and the radical angle is 110−112°, depending on the basis set. The corresponding comparison has not be made for the stannyl system, although *ab initio* calculations[45] predict that the stannyl radical has a H−Sn−H angle of 109−110°. The anions of the binary hydrides lower in the column are generally expected to have smaller H−M−H angles, as a result of an increase in the s−p splitting. This results in less orbital mixing, and the "extra" electron is in an orbital with substantial s character, making it more difficult to remove.

Because of differences in electronegativity, the first row anions retain more charge on the central atom than do those in rows 2 and 3. In addition, as noted above, symmetry also plays an important role. As suggested by the Mulliken population analysis from our Gaussian-type calculations,[46] in CH_3^- there is relatively little charge (~20%) on the hydrogens, while in SiH_3^- roughly 70% is on the hydrogens. The SiH_3^- anion is pyramidal and the "extra" electron is substantially delocalized onto the hydrogens. For anions with higher symmetry, e.g. PH_2^-, the HOMO must be nonbonding, and we expect less charge to be on the hydrogens. Thus, in NH_2^- the hydrogens are calculated to be slightly positive, and in PH_2^- only about 20% of the negative charge is on the hydrogens.

Bond Dissociation Energies. We can derive germanium−hydrogen and tin−hydrogen bond dissociation energies ($D°$(M−H)), from our acidities, electron affinities, and the ionization potential of hydrogen,[1] 313.6 kcal/mol; these are summarized in Table 3.

$$D°(Me_3M-H) = \Delta H°_{acid}(Me_3MH) + EA(Me_3M) - IP(H) \quad (8)$$

In column IVA, the $D°$(M−H) decreases down the column. The decreases in bond energies are nearly constant (13-15 kcal/mol) from row to row. Columns VA through VIIA also show bond energy decreases down the column.

The decrease in the bond dissociation energy down a column arises from the increased M radius and the resulting poorer M−H overlap. Across a row the bond energies are harder to predict. In general, we expect the bond energies to increase somewhat as the bonding atom becomes more electronegative.[32] Thus $D°(CH_4)$ = 105 kcal/mol, $D°(NH_3)$ = 107.4 kcal/mol, $D°(OH_2)$ = 119 kcal/mol, and $D°$(FH) = 136 kcal/mol.[33] Other factors, including ligation and changes in geometry for column IVA also are important so that $D°(CH_4)$ = 105 kcal/mol and $D°(NH_3)$ = 107.4 kcal/mol but $D°(SiH_4)$ = 91.6 kcal/mol and $D°(PH_3)$ = 83.9 kcal/mol, and $D°(GeH_4)$ = 80−86 kcal/mol and $D°(AsH_3)$ = 73.5 kcal/mol.[33]

Acidities. We compare the acidities of the hydrides from columns IVA through VIIA, and we note two trends. First, the acidities generally increase across a row of the periodic table ($\Delta H°_{acid}$(R−H) decreases): the acidity increases 45 kcal/mol from CH_4 to HF, 40 kcal/mol from SiH_4 to HCl, and 35 kcal/mol from GeH_4 to HBr. Second, the acidities increase down a column of the periodic table.[32,33] The increases for columns IVA (CH_4 to GeH_4), VA (NH_3 to AsH_3), VIA (H_2O to H_2Se), and VIIA (HF to HBr) are 58, 46, 41, and 48 kcal/mol, respectively.

Acidities are related to electron affinities and bond dissociation energies via the thermochemical cycle, eq 8, rewritten.

$$\Delta H°_{acid}(Me_3MH) = D°(Me_3M-H) - EA(Me_3M) + IP(H) \quad (9)$$

This relationship can be used to understand the relative contributions of electron affinity and bond dissociation energy to the acidity. Either an increase in the electron affinity or a decrease in the bond dissociation energy will cause the acidity to increase ($\Delta H°_{acid}$ decrease). Across a row of the periodic table, the increase in the acidity results from the large increases in the electron affinity.[32] The electron affinity increases from methyl to fluorine, silyl to chlorine, and germyl to bromine are 76, 51, and 37 kcal/mol, respectively. The bond dissociation energy also increases (31, 11, and < 8 kcal/mol, respectively), reducing the acidity increase. Down a column the acidity increase generally results from the large decrease in the bond dissociation energy. The bond dissociation energy decreases for columns IVA through VIIA are ~20 (CH_4 to GeH_4), 33 (NH_3 to AsH_3), 31 (H_2O to H_2S), and 48 (HF to HBr) kcal/mol, respectively. In column IVA, the large increase in the electron affinity (38 kcal/mol from methyl to germyl) also contributes to the acidity increase.[32,33,47] Interestingly, the

(39) Schulz, P. A.; Mead, R. D.; Jones, P. L.; Lineberger, W. C. *J. Chem. Phys.* **1982**, *77*, 1153.
(40) Hotop, H.; Lineberger, W. C. *J. Phys. Chem. Ref. Data* **1985**, *14*, 731.
(41) Janousek, B. K.; Brauman, J. I. *Phys. Rev. A* **1981**, *23*,
(42) Tack, L. M.; Rosenbaum, N. H.; Owrutsky, J. C.; Saykally, R. J. *J. Chem. Phys.* **1986**, *85*, 4222−4227.
(43) Albright, T. A.; Burdett, J. K.; Whanbo, M. H. *Orbital Interactions in Chemistry*; Wiley-Interscience: New York, 1985.
(44) Salzner, U.; Schleyer, P. v. R. *Chem. Phys. Lett.* **1992**, *199*, 267−274.
(45) Moc, J.; Rudzinski, M. M.; Ratajczak, H. *Chem. Phys.* **1992**, *159*, 197−210.
(46) Frisch, M. J.; Trucks, G. W.; Head-Gordon, M.; Gill, P. M. W.; Wong, M. W.; Foresman, J. B.; Johnson, B. G.; Schlegel, H. B.; Robb, M. A.; Replogle, E. S.; Gomperts, R.; Andres, J. L.; Raghavachari, K.; Binkley, J. S.; Gonzalez, C.; Martin, R. L.; Fox, D. J.; Defrees, D. J.; Baker, J.; Stewart, J. J. P.; Pople, J. A.; Gaussian 92, Revision B; Gaussian, Inc.: Pittsburgh PA, 1992.
(47) Berger, S.; Brauman, J. I. *J. Am. Chem. Soc.* **1992**, *114*, 4737−4743.

acidity behavior of column IVA is quite regular, despite the behavior of the electron affinities and the bond dissociation energies.

Methyl Substituents. In column IVA the electron affinities for the trimethyl-substituted compounds increase dramatically from row 1 to row 2 (EA(Me_3C) = −3.1 kcal/mol,[48] EA(Me_3Si) = 22.4 kcal/mol[2]), then more slowly for the other rows (EA(Me_3Ge) = 31.9 kcal/mol, EA(Me_3Sn) = 39.2 kcal/mol). A comparison of the unsubstituted hydride radicals and the methyl-substituted radicals (i.e., H_3Ge vs Me_3Ge) reveals that substitution of three methyl groups always decreases the electron affinity ~5−10 kcal/mol. This is consistent with the behavior seen for the other columns of the periodic table: EA(OH) = 41.1 kcal/mol,[39] EA(OMe) = 36.2 kcal/mol[49,50] and EA(SH) = 53.4 kcal/mol,[41] EA(SMe) = 43.2 kcal/mole.[51]

The $D°$(M−H) decreases down the column for the Me_3MH compounds, ~6−9 kcal/mol per row. Substitution of methyl groups for the hydrogens in the hydrides decreases the $D°$(M−H) for carbon ($D°(CH_4)$ = 104.8 kcal/mol vs $D°(Me_3CH)$ = 96.5 kcal/mol)[52] but appears to have essentially no effect in silyl[3,53,54] and perhaps a small effect in germyl. We do not have any data on stannane to compare with the trimethyltin hydride data. The available data[33] for elements in the other columns indicate that methyl substitution generally decreases the $D°$(M−H):[33] $D°(H_2O)$ = 119 kcal/mol vs $D°$(MeO−H) = 104 kcal/mol; $D°(NH_3)$ = 107.4 kcal/mol vs $D°(Me_2N-H)$ = 91.5 kcal/ mol.

The acidities in the trimethyl-substituted compounds increase down the column, as seen for the binary hydrides ($\Delta H°_{acid}(Me_3CH)$ = 413.1 kcal/mol,[48] $\Delta H°_{acid}(Me_3SiH)$ = 383 kcal/mol,[55] $\Delta H°_{acid}(Me_3GeH)$ = 362 kcal/mol, $\Delta H°_{acid}(Me_3SnH)$ = 349 kcal/mol). Similar behavior is also seen for the methyl-substituted compounds in the other columns.[33,47]

Because methyl substitution decreases both the electron affinity and the bond energy, but to varying extents, the substitution of methyl for hydrogen does not show a predictable effect on the acidities of the hydrides in columns VA through VIIA. In some cases the acidity increases ($\Delta H°_{acid}(H_2O)$ = 391 kcal/mol vs $\Delta H°_{acid}$(MeOH) = 380.6 kcal/mol), while in others the acidity decreases ($\Delta H°_{acid}(H_2S)$ = 351.2 kcal/mol vs $\Delta H°_{acid}$(MeSH) = 356.9 kcal/mol).[33] In the substituted methanes, methyl substituents generally increase the acidity, although substitution of the first methyl group decreases the acidity ($\Delta H°_{acid}(CH_4)$ = 416.6 kcal/mol , $\Delta H°_{acid}(CH_3CH_3)$ = 420.1 kcal/mol, $\Delta H°_{acid}(Me_2CH_2)$ = 419.4 kcal/mol, $\Delta H°_{acid}(Me_3CH)$ = 413.1 kcal/mol[48]). Methyl substitution in silane decreases the acidity of silane.[2,55] Methyl substitution in germane shows a similar acidity trend to that seen in the methanes: $\Delta H°_{acid}(GeH_4)$ = 359 kcal/mol,[56] $\Delta H°_{acid}(MeGeH_3)$ = 367 kcal/mol,[56] $\Delta H°_{acid}(Me_3GeH)$ = 362 kcal/mol).

The reported $\Delta H°_{acid}(MeGeH_3)$ seems to be higher than might have been expected. We can use this acidity and an estimate of the electron affinity of $MeGeH_2$ to estimate $D°$(Ge−H) for this compound. If we assume the electron affinity of $MeGeH_2$ is between that for GeH_3 (40.1 kcal/mol) and that for $GeMe_3$ (31.9 kcal/mol), we estimate that $D°$(Ge−H) is between 85 and 93 kcal/mol. This suggests that methyl substitution increases the $D°$(Ge−H), which does not fit the expected trend: methyl substitution in methane decreases the $D°$(C−H) 2 to 4 kcal/mol per substituted methyl[33,57] while methyl substitution in silane has essentially no effect on the $D°$(Si−H).[53] Our estimate of the $D°$(Ge−H) for Me_3GeH from our electron affinity and our acidity is consistent with methyl substitution causing either a small decrease or no change in the $D°$(Ge−H).

Summary

The electron affinities of trimethylgermanium and trimethyltin have been measured by electron photodetachment spectroscopy. The values of group IVA radicals provide an important contrast to those of the isoelectronic radicals in groups VA−VIIA. Some of the origins of the differences have been analyzed.

Acknowledgment. We are grateful to the National Science Foundation for support of this work. We thank Dr. Brian Wladkowski (NIST) for advice and help with the quantum calculations.

JA942228Q

(48) DePuy, C. H.; Gronert, S.; Barlow, S. E.; Bierbaum, V. M.; Damrauer, R. *J. Am. Chem. Soc.* **1989**, *111*, 1968−1973.
(49) Engelking, P. C.; Ellison, G. B.; Lineberger, W. C. *J. Chem. Phys.* **1978**, *69*, 1826.
(50) Janousek, B. K.; Zimmerman, A. H.; Reed, K. J.; Brauman, J. I. *J. Am. Chem. Soc.* **1978**, *100*, 6142−6148.
(51) Moran, S.; Ellison, G. B. *J. Phys. Chem.* **1988**, *92*, 1794−1803.
(52) Berkowitz, J.; Ellison, G. B.; Gutman, D. *J. Phys. Chem.* **1994**, *98*, 2744−2765.
(53) Walsh, R. *Acc. Chem. Res.* **1981**, *14*, 246−252.
(54) Allendorf, M. D.; Melius, C. F. *J. Phys. Chem.* **1992**, *96*, 428−437.
(55) Damrauer, R.; Kass, S. R.; DePuy, C. H. *Organometallics* **1988**, *7*, 637−640.
(56) Decouzon, M.; Gal, J.-F.; Gayraud, J.; Maria, P.-C.; Vaglio, G.-A.; Volpe, P. *J. Am. Soc. Mass Spectrom.* **1993**, *4*, 54−57.
(57) Seakins, P. W.; Pilling, M. J.; Niiranen, J. T.; Gutman, D.; Krasnoperov, L. N. *J. Phys. Chem.* **1992**, *96*, 9847−9855.
(58) Seetula, J. A.; Feng, Y.; Gutman, D.; Seakins, P. W.; Pilling, M. J. *J. Phys. Chem.* **1991**, *95*, 1658−1664.
(59) Ruscic, B.; Schwarz, M.; Berkowitz, J. *J. Chem. Phys.* **1990**, *92*, 1865−1875.